Dust as probe for horizontal field distribution in low pressure gas discharges

2014 Plasma Sources Sci. Technol. 23 045008

(http://iopscience.iop.org/0963-0252/23/4/045008)

IOP Publishing Plasma Sources Science and Technology

Plasma Sources Sci. Technol. **23** (2014) 045008 (7pp) doi:10.1088/0963-0252/23/4/045008

Dust as probe for horizontal field distribution in low pressure gas discharges

Peter Hartmann[1,2], Anikó Zs Kovács[1], Jorge C Reyes[2], Lorin S Matthews[2] and Truell W Hyde[2]

[1] Department of Complex Fluids, Institute for Solid State Physics and Optics, Wigner Research Centre, Hungarian Academy of Sciences, P O Box 49, H-1525 Budapest, Hungary
[2] Center for Astrophysics, Space Physics and Engineering Research (CASPER), One Bear Place 97310, Baylor University, Waco, TX 76798, USA

Received 20 February 2014, revised 6 May 2014
Accepted for publication 30 May 2014
Published 23 June 2014

Abstract

Using dust grains as probes in gas discharge plasma is a very promising, but at the same time very challenging method, as the individual external control of dust grains has to be solved. We propose and demonstrate the applicability of the RotoDust experiment, where the well controlled centrifugal force is balanced by the horizontal confinement field in plane electrode argon radio frequency gas discharges. We have reached a resolution of 0.1 V cm^{-1} for the electric field. This technique is used to verify numerical simulations and to map symmetry properties of the confinement in dusty plasma experiments using a glass box.

Keywords: dusty plasma, low pressure gas discharge, discharge diagnostics

(Some figures may appear in colour only in the online journal)

1. Introduction

Since the discovery and standard use of dusty plasmas, one of the most promising applications is the use of micron-sized solid particles as discharge probes. This concept is based on the assumption that the particles will settle at positions where the forces acting on them are in balance, and that a low enough dust number density (down to a single particle) will not alter the discharge conditions. At the same time, the dust particles are big enough to be easily observed by conventional video microscopy. After the formulation of the concept [1, 2], much effort has gone into the elaboration of the details of this technique in recent years [3–7], but it is still an exotic method with large, but untapped potential. For this technique to become widely useful, the issue of controlling the forces acting on the particles has to be solved.

A single dust particle immersed and charged in a low pressure gas discharge is exposed to a series of interactions, which include:

- gravity, $F_{\mathrm{G}} = mg$,
- electric field, $F_{\mathrm{E}} = qE$,
- magnetic field, $F_{\mathrm{M}} = q(\boldsymbol{v} \times \boldsymbol{B})$,
- ion drag, $F_{\mathrm{I}} \approx Zzn_i\alpha\boldsymbol{u}$,
- neutral drag $F_{\mathrm{N}} \approx -m\nu\boldsymbol{w}$,
- thermophoresis, $F_{\mathrm{T}} \approx 2.4n_{\mathrm{g}}\pi\lambda_{\mathrm{g}}(\partial T_{\mathrm{g}}/\partial \boldsymbol{r})$, etc.,

where m is the mass, $q = -eZ$ is the charge, and $\boldsymbol{v}$ is the velocity of the dust grain, $z = Ze^2/(4\pi\varepsilon_0 aT_{\mathrm{e}})$ is the dimensionless grain charge, T_{e} is the electron temperature, a is the grain diameter, n_i is the ion density, α is a phenomenological drag coefficient, $\boldsymbol{u}$ is the velocity of the ions relative to the grain, ν is the Epstein drag coefficient, $\boldsymbol{w}$ is the grain velocity relative to the background gas, n_{g} is the density of the background gas, λ_{g} is the collisional mean free path of the background gas atoms and T_{g} is the gas temperature. Extensive discussions of all these interactions and the dust particle charging can be found in [5, 8].

The order of importance of the interactions listed above strongly depends on the local discharge conditions at the position of the dust particle. For instance, in the sheath region of a radio frequency (RF) noble gas discharge, the levitation height is mostly determined by the balance of gravity and the strong sheath electric field, while in the bulk of an RF discharge under microgravity conditions, the observed dust void forms due to the strong ion drag effect [9].

The limitations of using a dust grain as a plasma probe originate from the fact that once it is released into the plasma, we lose control over its properties, like electric charge (surface potential) and position in the plasma. An important capability is to change our possibilities from simply observing the particle to being able to manipulate it in a controlled manner.

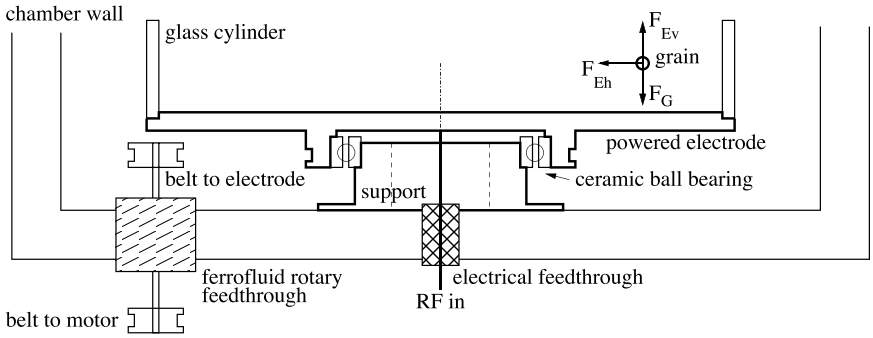

Figure 1. Schematics of the 'RotoDust' electrode configuration. The main forces of interest: gravity, horizontal and vertical components of the electric field are illustrated acting on a representative dust grain.

Laser manipulation, being an extremely successful technique in other branches of dusty plasma research [10–12], provides a possibility to push individual dust grains; however, the force introduced by the radiation pressure of a laser beam on a grain can only be estimated (rather inaccurately) and poorly controlled over an extended period of time.

A different, more promising direction seemed to be to modify the gravitational force F_G. An obvious way of realizing this is to change the mass of the particle by simply choosing different sized dust grains. Practical reasons limit the dust size in the range of $1 < a < 50\,\mu$m. Smaller particles are undetectable, while bigger particles are too heavy to be levitated by the fields in the discharge. Changing the physical conditions of the grain e.g. from solid to hollow may extend the size range a bit. More innovative approaches target the gravitational acceleration constant g. Micro-gravity experiments on parabolic flights and the International Space Station (ISS) can practically reach $g \approx 0\,\mathrm{m\,s^{-2}}$ [13, 14]. Alternatively, hyper-gravity experiments in centrifuges could increase the gravitational acceleration up to $g \approx 26.5\,\mathrm{m\,s^{-2}}$ [15]. These methods make it possible to move the dust across the discharge from the central, practically electric field free region to deep into the high field sheath (edge) plasma in a controlled way. Both methods share the advantage that the discharge plasma is largely unaffected while the dust grain is moved, however, they rely on very expensive and widely inaccessible infrastructure, making each experiment unique and practically irreproducible.

Here we propose a new method to measure the horizontal electric field in typical RF low pressure gas discharges with electrode configurations symmetric around a vertical axes. In section 2 the experimental method and setup are described in detail, in section 3 the experimental results are presented and verified against simulation results, and an example for application is given, followed by a short summary in section 4.

2. Experimental method

Our method of introducing a well controlled external force to the dust grain in the discharge plasma utilizes the centripetal force, which keeps a particle gyrating around a fixed center on a circular orbit. The rotation is introduced externally, while the centripetal force is provided by the horizontal component of the electric field inside the discharge.

The experiments were performed in our dusty plasma setup already introduced in [16]. The lower electrode has been modified according to figure 1, showing the schematic sketch of our 'RotoDust' setup [17]. An adjustable speed dc motor was used to drive the powered electrode through a ferrofluid rotary feedthrough and Viton belts. The angular velocity of the rotating electrode could be continuously adjusted in the range $0 \leqslant \Omega < 25\,\mathrm{rad\,s^{-1}}$. The rotating electrode drags the background gas above it and induces rotation of the gas. The rotating gas, on the other hand, drags the dust particles, resulting in a stable rotation of the dust component, which builds up in a few seconds after switching on the rotation. Due to the low pressure in the 1 Pa range used in our experiments, it is safe to assume that turbulence does not develop. Also it seems to be certain that this rotation of the background gas does not affect the plasma properties, because electron and ion transport in these discharges happens on the sub micro-second timescale, and the uncorrelated thermal velocity of the background gas atoms exceeds the rotation speed by about 3 orders of magnitude at room temperature.

During the measurement, we introduce a single, size-certified spherical melamine-formaldehyde (MF) dust particle into the discharge, switch on rotation at a given, constant angular velocity Ω and measure the radius R of the stable circular orbit of the dust particle. In this case, observing the motion from the laboratory frame, the centripetal force, which is purely horizontal, is provided by the horizontal component of the confinement electric field E_{conf} at a radial position R:

$$q\,E_{\mathrm{conf}}(R) = m R \Omega^2. \tag{1}$$

All factors on the right hand side of (1) are known or measured with high precision, thus the product of the electric charge of the grain and the confinement field strength is found with the same high precision. As a consequence, absolute field strength measurements are as accurate as the grain charge estimate is accurate, which is typically in the 10–20% range. For relative field measurements, however, the stability of the grain charge is important, while its absolute value together with its uncertainty is irrelevant, resulting in significantly better relative accuracy. To estimate the sensitivity of this method we assume typical values of dust grain mass ($m \approx 10^{-13}$ kg

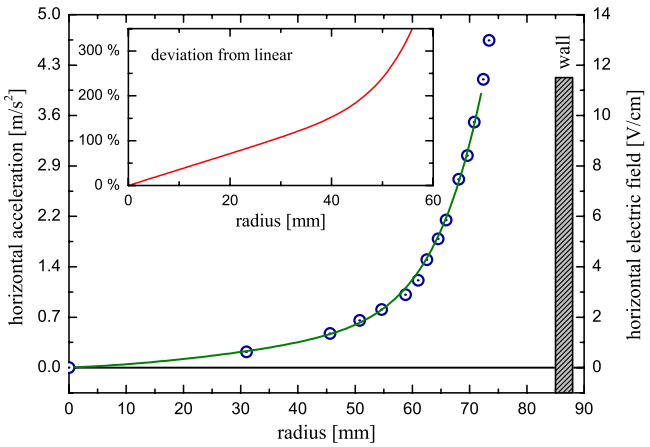

Figure 2. Measured radial distribution of the horizontal centripetal acceleration (left scale) and electric field (right scale). Lines represent polynomial fits, see text for details. The inset shows the ratio of higher order and the first order terms of the fitted polynomial.

for a grain with 5 μm diameter) and charge ($Z \approx -10^4 e$) based on earlier experiments. Further assuming angular velocities in the range of 1 rad s^{-1} and orbit radii in the range of centimeters, the detectable electric fields are in the order of V m^{-1} (or 10^{-2} V cm^{-1}). This sensitivity exceeds that of every conventional diagnostic technique (e.g. electric probes, Stark spectroscopy, etc.), by orders of magnitude. This enhanced sensitivity makes this technique attractive for many applications and drives recent developments, including the present work.

3. Results and application

In the first experiment, which targets the demonstration and validation of the method, we have used MF dust grains with $a = 9.16\,\mu$m diameter ($m = 6.03 \times 10^{-13}$ kg), which were inserted into a 13.56 MHz, radio frequency (RF), $p = 1.0$ Pa pressure argon gas discharge, absorbing 8 W of RF power with peak-to-peak voltage of $V_{pp} = 175$ V. The lower, flat, horizontal, powered electrode had a glass ring of $R_{wall} = 85$ mm inner radius and $H = 100$ mm height at its edge. The top plate of the grounded vacuum chamber was 120 mm above the powered electrode.

During the actual measurements a few (<10) particles were dropped into the discharge. After setting a stable rotation speed, the orbital radii were measured with the aid of a laser source mounted on a linear translator stage. The raw measured quantities are the angular velocities Ω and radii of the orbiting particles R. From these the centripetal acceleration $g_{centr} = R\Omega^2$ and further the horizontal confinement electric fields are derived by applying equation (1) (see figure 2).

As expected, at rest ($\Omega = 0$) the equilibrium position of our dust grains is at the center. Slowly increasing the rotation rate, the grains are observed to react very sensitively, indicating a very weak confinement force near the center. To approach the glass wall, which is negatively charged, much higher rotation rates are needed. In this case we have reached rotation rates up to 1.8 rot s^{-1} ($\Omega = 11.3$ rad s^{-1}). In figure 2 a polynomial fit in the form $E_{conf}(R) \approx c_1 R + c_2 R^2 + c_9 R^9$ is also shown, which is used for further analysis. First we test the assumption, often made while discussing trapped systems, that the trap can be modeled by a harmonic potential close to the center. The inset in figure 2 shows the ratio $(c_2 R^2 + c_9 R^9)/(c_1 R)$, quantifying the deviation of the measured force field from an ideal harmonic trap (which has a linear force field). We see that at $R \approx 25$ mm ($R/R_{wall} \approx 0.3$) the second order contribution becomes equal to the linear term and above $R \approx 45$ mm ($R/R_{wall} \approx 0.5$) the higher order term dominates.

The most critical unknown parameter linking the centripetal acceleration to the electric field (left and right scales of figure 2) is the charge of the dust grain. First of all, we assume the charge is constant and independent of the radial coordinate R. This approximation will obviously fail very close to the glass wall, but the radial extent for which this assumption is valid will be discussed later. Second, we have to quantify the electric charge of the dust grain. Luckily, over the past two decades of intensive dusty plasma research, several experimental and theoretical methods have been developed to do this. In reference [17] we describe the application of two experimental methods. In the case of a large plasma crystal, the fluctuation spectra are used to determine the charge, while in the case of a two particle system, the center of mass and inter-particle oscillations are used to extract the charge. Both of these methods rely on particle tracking velocimetry (PTV) [18] and the assumption of screened Coulomb (Yukawa) type inter-particle forces. This approximation is widely accepted and confirmed in the case of (horizontal) single layer configurations, but it is known to fail in the vertical direction due to streaming of charged plasma particles. Based on our experience with our experimental setup, we estimate $Z = q/e = -12000 \pm 2500$ in the current experiment, but this estimate will be refined later in this manuscript. For alternative methods and discussions see e.g. [19, 20].

From the theoretical side, for the discharge conditions relevant to dusty plasma experiments, the orbital motion limited (OML) analytical method is preferred for calculating the charge over other approaches, like the diffusion limited model (DLM) or the radial drift model (RDL). For detailed discussion and derivation of these approaches, see [8]. Besides analytical models, phenomenological approximations and numerical simulations can also be applied to calculate the dust grain charge [21–23].

3.1. Numerical simulation

One of the most promising applications of using dust grains as plasma probes is to use experimentally obtained electric field data to validate numerical simulations, where the electric field (through the potential) is usually one of the principle quantities implicitly calculated during the simulations. To demonstrate the power of this technique, we have modified our 'particle-in-cell with Monte Carlo collisions' (PIC/MCC) code [24], which has been validated and benchmarked in a multi-group collaboration [25]. We have extended it to describe cylindrically symmetric finite discharges, including wall charging and electron–argon

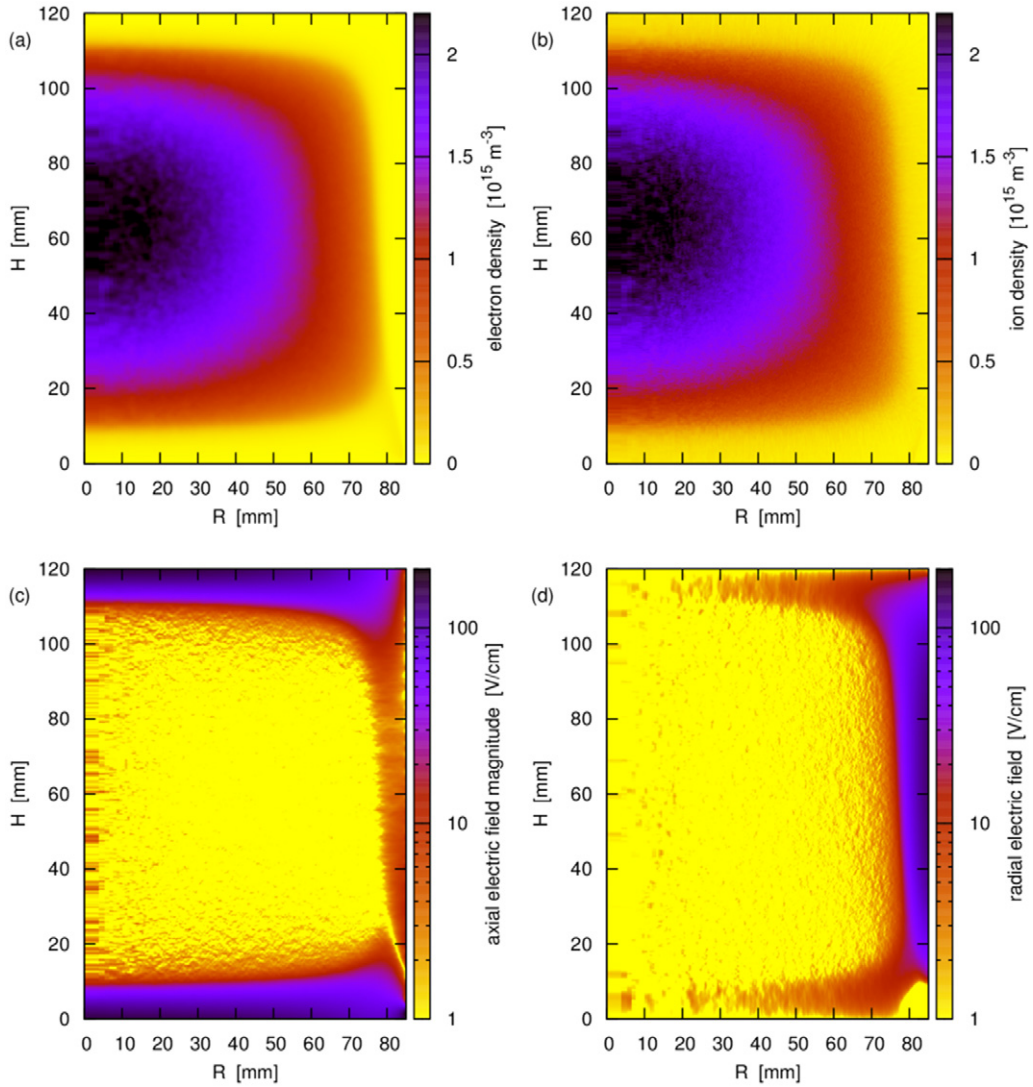

Figure 3. Cylindrical PIC/MCC simulation results: (*a*) electron density, (*b*) Ar^+ ion density, (*c*) magnitude (absolute value) of the axial electric field, and (*d*) radial electric field. Horizontal axis shows the radial distance from the center, while the vertical axis runs from the lower, powered electrode to the grounded top electrode of the discharge. The distributions are averaged over ten RF cycles.

collisions [26, 27]. The description of all details of this simulation code goes well beyond the scope of this paper, here we give only a brief introduction. The simulation results have been calculated using our electrostatic 2d(R,H)3v PIC/MCC code. We restricted the simulation volume to the relevant region inside the confining glass cylinder, which is placed at the electrode edge (see figure 1). Input parameters were set based on the experiment: Voltage amplitude = 170 V at 13.56 MHz, Argon pressure = 1 Pa, gas temperature = 400 K. The superparticles of the PIC simulation had a constant weight of 80 000 for both electrons and Ar^+ ions, the computational grid was set to represent constant volume cells and had a size of 512×512. The electrostatic Poisson's equation was solved in every time-step using the combined Fourier (in H) and direct space (in R) method described in [28]. Computational speedup was achieved by implementing MPI parallelization. It should be noted that PIC/MCC simulations have already been successfully used to compute forces acting on dust particles of different geometries, as in [29, 30].

Figure 3 shows time averaged distributions of electron and ion densities, and the axial and radial electric fields. The presence of a large density, practically field free bulk plasma is the most prominent feature, clearly visible in the figures. This bulk plasma is surrounded by boundary layers, referred to as plasma sheaths, on all sides. The axial electrode sheath is a well studied feature, accurately described by earlier simulations and analytical models [31, 32]. Most relevant here are panels (*c*) and (*d*), as the axial field is responsible for the levitation of the dust grain through the simple relation

$$q\boldsymbol{E}_{\mathrm{axial}}(H) + m\boldsymbol{g} = 0, \tag{2}$$

expressing vertical force balance at vertical position H, while the radial field yields the confinement.

Here we return to two questions posed above related to the dust grain charge. Our first assumption was that the charge is independent of the radial position R. From figures 3(*a*) and (*b*) we can see that at the lower sheath edge (around $10 < H < 15$ mm height) the charged particle densities

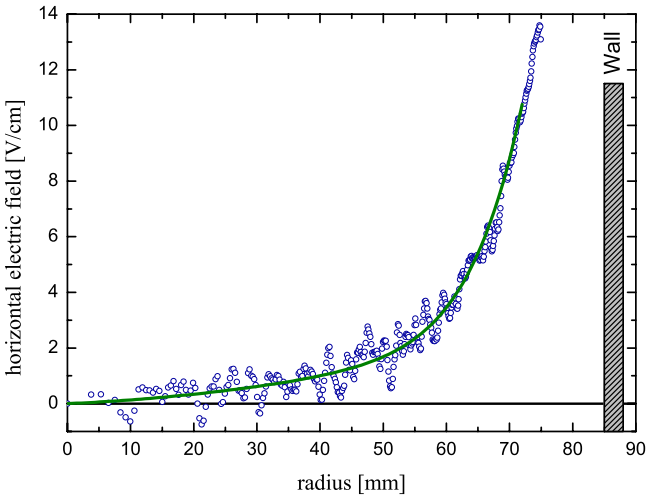

Figure 4. Comparison of the radial electric field obtained from the experiment (solid line, same as in figure 2) and the PIC/MCC simulation (circles, same as in figure 3(*d*)).

(relevant for the charging process) are fairly constant up to $R \approx 75$ mm, supporting our assumption and the results shown in figure 2.

To refine our first estimate for the dust grain charge, we iteratively converge its value appearing in equations (1) and (2) using the data from our PIC/MCC simulation for the electric field components, and the measured centripetal acceleration data. This procedure results in the levitation height $H(R)$ and the constant charge q.

Figure 4 shows the comparison between the measured and the computed radial electric field. Remarkable agreement can be seen. We have to emphasize that the only free linear scaling parameter is the electric charge of the dust grain, which was found to be $Z = q/e = -13500 \pm 500$, which is consistent with our first estimate.

3.2. Glass box application

After having demonstrated the consistency of our experimental and numerical results, we apply this method to an experimental system frequently used since the discovery of Yukawa balls [33], which are spherical (three dimensional) ensembles of dust particles with interesting new features, like ordered shell structures [34] and anisotropic melting properties [35], and other vertical dust structures [36]. Common to these experiments is the use of an open (on top and bottom) glass box to modify the confinement field and other plasma parameters. In principle, from point of view of symmetry, the use of a cylinder instead of the box would be more appropriate, but due to practical experimental reasons a glass cylinder, which would induce unwanted distortions in the optical tracking of the grains, is clearly not preferred. For our numerical simulations, however, the glass box has to be replaced by a cylinder, otherwise a full three-dimensional PIC/MCC simulation would be needed, which requires extraordinary computational resources. Luckily, most glass box experiments report principally spherically or cylindrically symmetric dust ensembles. It seems to be controversial that

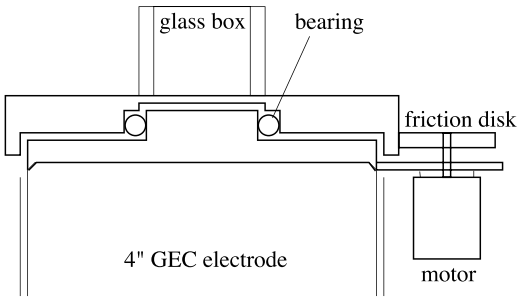

Figure 5. Schematics of the rotatable extension placed on the standard 4 inch electrode column of the GEC reference cell.

spherical structures are formed in a field which is determined by cubic boundary conditions. We have conducted an experiment campaign with the aim to map the field inside a glass box more precisely to show the transition from the cylindrical to rectangular symmetry of the confinement field inside the glass box.

To realize this experiment we have modified the dusty plasma setup at the Hypervelocity Impacts and Dusty Plasmas Lab (HIDPL) of the Center for Astrophysics, Space Physics, and Engineering Research (CASPER) at Baylor University, Waco, Texas. Detailed description of the setup is given in [37]. We have added a rotatable extension to the powered lower electrode, driven by a small dc motor directly attached to it, as schematically shown in figure 5. A glass box with inner side length $L = 18$ mm was fixed centered on top of the rotatable electrode disc. The argon discharge at a pressure of $p = 20$ Pa was driven by 10 Watts of RF power. Dust grains with diameter $a = 6.5\,\mu$m were inserted into the box forming a small, cylindrically symmetric single layer plasma crystal.

Figure 6 shows examples of particle snapshots at three different rotation rates. The video sequences were taken from the top at 125 frames per second (fps) with a short exposure time of 1/5000 s. At slow rotation speeds the dust cloud extends radially outward and shows a cylindrically symmetric structure, while at fast rotation, the cloud extends further towards the walls of the glass box, where the confinement field approaches a rectangular symmetry. To quantify the anisotropy, we measure the apparent diameter of the dust cloud along directions parallel to the glass box walls (D_1) and its diagonal (D_2). The ratio of these two diameters is plotted in figure 7 versus the ratio D_2/L ratio.

Based on these results we conclude that (at least under the particular condition of this experiment) dust particles inside the glass box, situated within the central 40% of the linear glass box side length, experience a cylindrically symmetric confinement field. Further out of this region the confinement field starts following the square symmetry of the glass box. The use of a glass cylinder, replacing the box, would provide symmetric confinement over the whole radial extent, while the detection could be performed with our new, single camera 3D imaging method [38], which could observe the dust cloud from the top, as it is done in traditional single layer experiments.

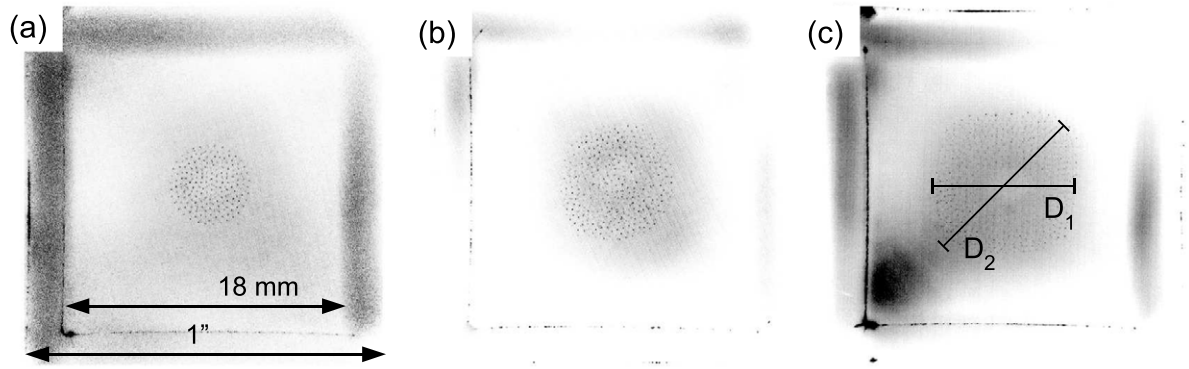

Figure 6. Inverted snapshots of the rotating glass box experiments. The rotation speeds are (*a*) 0 rot s^{-1}, (*b*) 2.66 rot s^{-1} and (*c*) 4.0 rot s^{-1}. In addition in (*a*) the dimensions are shown, while in (*c*) the parallel and diagonal diameters are illustrated.

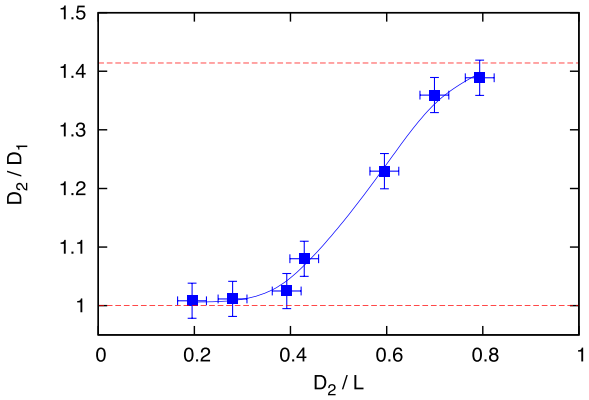

Figure 7. Asymmetry parameter D_2/D_1 versus the ratio of the diagonal diameter to box the side length. Lower and upper dashed lines indicate theoretical limits.

4. Summary

With the RotoDust setup, shown schematically in figure 1, we are able to continuously scan over the horizontal levitation plane of the dust grain and precisely measure the distribution of the horizontal (confinement) field experienced by the dust grains. In our first experiment we have demonstrated a sensitivity of approximately 0.1 V cm^{-1} in electric field measurements. Comparison with our cylindrically symmetric PIC/MCC simulation resulted in excellent agreement between experimental and numerical results with only a single linear scaling parameter, the dust grain charge. The RotoDust principle was used to show the size limit where cylindrically symmetric confinement fields in glass box experiments can be expected.

Acknowledgment

This research has been supported by the OTKA Grant NN-103150.

References

[1] Tomme E B, Annaratone B M and Allen J E 2000 Damped dust oscillations as a plasma sheath diagnostic *Plasma Sources Sci. Technol.* **9** 87

[2] Samarian A A and James B W 2005 Dust as fine electrostatic probes for plasma diagnostic *Plasma Phys. Control. Fusion* **47** B629

[3] Basner R, Sigeneger F, Loffhagen D, Schubert G, Fehske H and Kersten H 2009 Particles as probes for complex plasmas in front of biased surfaces *New J. Phys.* **11** 013041

[4] Maurer H R, Schneider V, Wolter M, Basner R, Trottenberg T and Kersten H 2011 Microparticles as plasma diagnostic tools *Contrib. Plasma Phys.* **51** 218–27

[5] Beckers J 2011 Dust particle(s) (as) diagnostics in plasmas *PhD Thesis* Technische Universiteit Eindhoven

[6] Carstensen J, Jung H, Greiner F and Piel A 2011 Mass changes of microparticles in a plasma observed by a phase-resolved resonance method *Phys. Plasmas* **18** 033701

[7] Schubert G, Haass M, Trottenberg T, Fehske H and Kersten H 2012 Plasma sheath structures in complex electrode geometries *Contrib. Plasma Phys.* **52** 827–35

[8] Tsytovich V N, Morfill G E, Vladimirov S V and Thomas H M 2008 *Elementary Physics of Complex Plasmas* (*Lecture Notes Physics* vol 731) (Berlin: Springer)

[9] Wolter M, Melzer A, Arp O, Klindworth M and Piel A 2007 Force measurements in dusty plasmas under microgravity by means of laser manipulation *Phys. Plasmas* **14** 123707

[10] Stoffels E, Stoffels W W, Vender D, Kroesen G M W and de Hoog F J 1994 Laser-particulate interactions in a dusty rf plasma *IEEE Trans. Plasma Sci.* **22** 116–21

[11] Melzer A 2001 Laser manipulation of particles in dusty plasmas *Plasma Sources Sci. Technol.* **10** 303–10

[12] Schneider V and Kersten H 2013 On the use of optically trapped dust particles as micro-probes in process plasmas *Problems At. Sci. Technol.* **2013** 164–7

[13] Fortov V E, Nefedov A P, Vaulina O S, Petrov O F, Dranzhevski I E, Lipaev A M and Semenov Yu P 2003 Dynamics of dust grains in an electron-dust plasma induced by solar radiation under microgravity conditions *New J. Phys.* **5** 102

[14] Thomas H M *et al* 2008 Complex plasma laboratory pk-3 plus on the international space station *New J. Phys.* **10** 033036

[15] Beckers J, Ockenga T, Wolter M, Stoffels W W, van Dijk J, Kersten H and Kroesen G M W 2011 Microparticles in a collisional rf plasma sheath under hypergravity conditions as probes for the electric field strength and the particle charge *Phys. Rev. Lett.* **106** 115002

[16] Hartmann P, Sándor M C, Kovács A Z and Donkó Z 2011 Static and dynamic shear viscosity of a single-layer complex plasma *Phys. Rev.* E **84** 016404

[17] Hartmann P, Donkó Z, Ott T, Kählert H and Bonitz M 2013 Magnetoplasmons in rotating dusty plasmas *Phys. Rev. Lett.* **111** 155002

[18] Feng Y, Goree J and Liu B 2007 Accurate particle position measurement from images *Rev. Sci. Instrum.* **78** 053704

[19] Sharma S K, Kalita R, Nakamura Y and Bailung H 2012 Dust charge measurement in a strongly coupled dusty plasma produced by an rf discharge *Plasma Sources Sci. Technol.* **21** 045002
[20] Carstensen J, Greiner F and Piel A 2010 Determination of dust grain charge and screening lengths in the plasma sheath by means of a controlled cluster rotation *Phys. Plasmas* **17** 083703
[21] Miloch W J, Vladimirov S V, Pécseli H L and Trulsen J 2009 Charging of insulating and conducting dust grains by flowing plasma and photoemission *New J. Phys.* **11** 043005
[22] Douglass A, Land V, Matthews L S and Hyde T W 2011 Dust particle charge in plasma with ion flow and electron depletion near plasma boundaries *Phys. Plasmas* **18** 083706
[23] Miloch W J and Block D 2012 Dust grain charging in a wake of other grains *Phys. Plasmas* **19** 123703
[24] Donkó Z 2011 Particle simulation methods for studies of low-pressure plasma sources *Plasma Sources Sci. Technol.* **20** 024001
[25] Turner M M, Derzsi A, Z. Donkó, Eremin D, Kelly S J, Lafleur T and Mussenbrock T 2013 Simulation benchmarks for low-pressure plasmas: capacitive discharges *Phys. Plasmas* **20** 013507
[26] Phelps A V 1994 The application of scattering cross sections to ion flux models in discharge sheaths *J. Appl. Phys.* **76** 747–53
[27] Phelps A V and Petrovic Z L 1999 Cold-cathode discharges and breakdown in argon: surface and gas phase production of secondary electrons *Plasma Sources Sci. Technol.* **8** R21
[28] Chao E H, Paul S F, Davidson R C and Fine K S 1997 Direct numerical solution of poisson's equation in cylindrical (r,z) coordinates *Technical Report* PPPL-3251 Princeton Plasma Physics Laboratory
[29] Schweigert I V, Alexandrov A L, Ariskin D A, Peeters F M, Stefanović I, Kovačević E, Berndt J and Winter J 2008 Effect of transport of growing nanoparticles on capacitively coupled rf discharge dynamics *Phys. Rev.* E **78** 026410
[30] Schubert G, Basner R, Kersten H and Fehske H 2011 Determination of sheath parameters by test particles upon local electrode bias, plasma switching *Eur. Phys. J.* D **63** 431–40
[31] Schulze J, Donkó Z, Heil B G, Luggenhölscher D, Mussenbrock T, Brinkmann R P and Czarnetzki U 2008 Electric field reversals in the sheath region of capacitively coupled radio frequency discharges at different pressures *J. Phys. D: Appl. Phys.* **41** 105214
[32] Schulze J, Schngel E, Donkó Z and Czarnetzki U 2011 The electrical asymmetry effect in multi-frequency capacitively coupled radio frequency discharges *Plasma Sources Sci. Technol.* **20** 015017
[33] Arp O, Block D, Bonitz M, Fehske H, Golubnychiy V, Kosse S, Ludwig P, Melzer A and Piel A 2005 3d coulomb balls: experiment and simulation *J. Phys.: Conf. Ser.* **11** 234
[34] Baumgartner H, Kählert H, Golobnychiy V, Henning C, Käding S, Melzer A and Bonitz M 2007 Shell structure of yukawa balls *Contrib. Plasma Phys.* **47** 281–90
[35] Schella A, Miksch T, Melzer A, Schablinski J, Block D, Piel A, Thomsen H, Ludwig P and Bonitz M 2011 Melting scenarios for three-dimensional dusty plasma clusters *Phys. Rev.* E **84** 056402
[36] Kong J, Hyde T W, Matthews L S, Qiao K, Zhang Z and Douglass A 2011 One-dimensional vertical dust strings in a glass box *Phys. Rev.* E **84** 016411
[37] Boessé C M, Henry M K, Hyde T W and Matthews L S 2004 Digital imaging and analysis of dusty plasmas *Adv. Space Res.* **34** 2374–8
[38] Hartmann P, Donkó I and Donkó Z 2013 Single exposure three-dimensional imaging of dusty plasma clusters *Rev. Sci. Instrum.* **84** 023501